Title

Formulation and Quality Consideration of Cannabidiol Printed Forms Produced by Fused-Deposition Modeling

Author names and affiliations

Olivier Jennotte*, Nathan Koch, Anna Lechanteur, Brigitte Evrard

Laboratory of Pharmaceutical Technology and Biopharmacy, Department of Pharmacy, Center for Interdisciplinary Research on Medicines (CIRM), University of Liege, 4000 Liege, Belgium

Corresponding author

*Olivier Jennotte (ojennotte@uliege.be)

Present/permanent address

*CHU, Tower 4, 2nd floor, Laboratory of Pharmaceutical Technology and Biopharmacy, Department of Pharmacy, University of Liege, Quartier Hôpital, Avenue Hippocrate 15, 4000 Liege, Belgium

Tel: 003243664307

Formulation and Quality Consideration of Cannabidiol Printed Forms Produced by Fused-Deposition Modeling

Olivier Jennotte, Nathan Koch, Anna Lechanteur, Brigitte Evrard

Laboratory of Pharmaceutical Technology and Biopharmacy, Department of Pharmacy, Center for Interdisciplinary Research on Medicines (CIRM), University of Liege, 4000 Liege, Belgium.

1. Introduction

Cannabidiol (CBD) is a promising non-psychoactive cannabinoid that shows several clinical outcomes. Commercially, this molecule is used in Epidiolex® (Greenwich Biosciences, Inc), a Food and Drug Administration (FDA)-approved drug to treat Lennox-Gastaut and Dravet syndromes, which are childhood-onset epilepsy [1]. These two syndromes are difficult to treat and the dosage of Epidiolex® can reach a maximum of 10 mg/kg twice a day [2]. In addition to these indications, CBD has been studied for the treatment of different health problems, such as opioids use disorder, social anxiety, schizophrenia or cancers with a wide range of dosages varying from less than 1mg/kg/day to 50 mg/kg/day [3–5]. For example, Hurd *et al.* recently performed a clinical trial to assess the efficacy of CBD to inhibit the drug cue-induced craving and anxiety in drug-abstinent individuals with heroin use disorder [6]. Moreover, some authors conducted a systematic review of clinical studies performed on CBD [7]. It first appeared that the tested CBD formulations were mainly administrated in the form of an oily solution, formulated in capsule or not. However, lipid formulations suffer from some drawbacks such as the sensitivity to oxidation or the compatibility with the capsule when encapsulation is considered [8]. The development of an oral solid dosage form of CBD would therefore be interesting for future investigations on its therapeutic effects. Secondly, among the trials that demonstrated positive effects of CBD on the treatment studied, the authors observed that the dosage of CBD can induce the variation of its therapeutic effect. Although clinical trials need to be conducted on a larger number of subjects, this suggests that in the future, clinicians will need to be able to formulate CBD drugs with adjustable dosages in order to be able to treat patients in the most effective way. In addition to these variable dosage challenges, the low bioavailability of CBD must be considered. Indeed, CBD is part of class II of the Biopharmaceutical Classification System (BCS). This drug shows poor aqueous solubility (0.01 µg/mL) and a high hepatic first pass metabolism which result in an estimated bioavailability of 6% [9]. Moreover, CBD absorption is erratic, leading to high variation of plasmatic concentrations in clinical population [10–12]. It is therefore crucial to develop strategies that improve CBD oral bioavailability with solid oral formulations which are preferred by patients and more stable than the liquid formulations.

Several techniques are used to improve the solubility of BCS II molecules, such as dissolution of the drug in lipid media, complexation into cyclodextrins, the impregnation of mesoporous silica or the formation of amorphous solid dispersions (ASDs), especially by hot-melt extrusion (HME) and spray drying [13–15]. Compared to the spray drying technique, HME has the advantage of working without the use of expensive and polluting solvents.

In a previous study, twin screw HME has already been used to increase the apparent aqueous solubility of CBD [16]. This technique involves the heating of a mixture between an active pharmaceutical ingredient (API) and one or more polymers along two screws, inside a barrel, until obtaining a filament in the shape of a spaghetti or a film, depending on the shape of the die. The filament can further, among other processes, be pelletized and filled into capsules, used directly as implant, be milled and compressed or shaped by 3D printing [17–20].

Since the FDA-approval of the first 3D printed dosage form Spritam® manufactured using the drop-on-powder deposition (Aprecia Pharmaceuticals), the application of 3D printing has been extensively studied in the pharmaceutical field. 3D printing represents a great potential in drug formulation due to its flexibility, its ability to produce very complex structures, amorphous forms, dosage forms with multiple drugs without drug-drug incompatibility issues and on-demand manufacturing [21]. In addition, 3D printing makes it possible to move away from the one-size-fits-all manufacturing approach applied by conventional manufacturing techniques. Due to differences in genetics, weight, height, metabolism, health condition, age and tendency for compliance from patient to patient, there is a need for drugs with adaptable drug combinations, dosages and release rates to treat each individual adequately [20,22]. Therefore, the faculty of 3D printing to convert a great number of digital patterns into solid drug dosage forms with different dose or drug release makes 3D printing a great tool in personalized medicine. In this regard, fused deposition modeling (FDM) has already offered solutions to many challenges. This technique consists of driving a filament by two wheels into a print head in which it is melted. The molten filament is deposited, layer by layer, on a platform until obtaining a 3D object, previously designed on a computer [23]. FDM has been reported for the print multiple layered tablets, each layer with a different drug to reduce the risk of a missing dose by the patient [24]. In another study, attractive shapes were printed by FDM to increase the compliance of young patients [25]. Another example is the use of FDM to manufacture pulsatile delivery system to treat patients suffering from conditions that require complex release profile [26]. Moreover, it's a low cost and simple method and it does not imply the use of organic solvents. These advantages could one day widespread decentralized drug manufacture by FDM, such as in hospitals or public pharmacies in which its advantages regarding the personalized medicine could be fully exploited. However despite the myriad of studies on the benefits of the 3D printing technique, there are still no guidelines regarding the evaluation of the performances or the quality control of the final 3D printed product [27]. Currently, the FDA recommends following the same production and control guidelines as conventional manufacturing techniques [28].

Therefore, this work aims to explore the development of a solid oral form of CBD with an immediate release printed by FDM. We have focused our research on the influence of the composition and the morphology of the formulation on the reproducibility of the process as well as on its pharmaco-technical performances based on the European Pharmacopoeia uncoated tablets monograph.

This study is divided into three parts. First, different combinations of two polymers mixed with CBD were extruded and printed in order to select the most suitable for the production of CBD

printed forms with an immediate release (IR).According to the European Pharmacopoeia, an IR is achieved if at least 80% of the drug is released within 45 min (European Pharmacopoeia, Edition 11.0, monograph 5.17.1). This type of formulation should increase the CBD bioavailability. Indeed, Izgelov claimed that, due to its lipid nature, absorption of CBD mainly occurs in the upper part of the intestine, explaining the advantage of the dissolution of the drug in the stomach [29]. In this regard, IR formulation were chosen as they should dissolve early in the gastrointestinal tract, making dissolved CBD available to be absorbed early in the intestine. Secondly, the selected formulation was extruded and printed in six different designs and the influence of the morphology was evaluated in terms of reproducibility and quality. Finally, the dosage adaptability allowed by the FDM was studied. In this regard, three different dosages of CBD were characterized and compared.

2. Material and methods

2.1. Materials

CBD was purchased from THC Pharm (Frankfurt, Germany). Eudragit®EPO (EPO, amino alkyl methacrylate copolymer, Tg: 50 °C, soluble in water at pH<5, gifted by Evonik, Germany) was used as matrix former. Poly ethylene oxide (PEO, POLYOX® WSR N10, MW 100000, gifted by Colorcon, UK), a semi-crystalline polymer (Tg = -67 °C and Tm = 65-70 °C) was used for its plasticizing effect.

2.2. Thermogravimetric Analysis (TGA)

TGA analysis were performed on CBD, EPO and PEO using Mettler-Toledo® TGA2 (Schwerzenbach, Swiss) controlled by the STARe System software version 12.10. Samples between 7 and 13 mg were added to an aluminum pan without lid. The % mass loss of CBD was measured during a heating ramp ranging from 25 to 500 °C at a rate of 20 °C/min. The experiments were conducted under nitrogen gas flow of 80 mL/min.

2.3. Drug Loaded Filaments Preparation

Five EPO/PEO ratios, added with 10% of CBD, were used to produce filaments by HME in order to select the formulation that allows the higher dissolution rate of CBD (Table 1). The physical mixtures were prepared using a mortar and a pestle and extruded using a Pharma 11 twin-screw extruder (ThermoFisher Scientific, Germany) with a screw configuration containing two kneading zones at 140 °C and 50 rpm. Two devices were set up in the extrusion line in order to modulate the filament diameter. The first one is a melt pump 12/3 (Advanced Futur Polymer, France), heated at 140 °C, connected between the barrel and the die. This pump is composed of two toothed wheels which decreased the pulsation output of the filament at the die. The second device is an air-cooled conveyor belt (ThermoFisher Scientific, Germany) which pulled the filament more or less quickly in order to decrease or increase the diameter of the filament. A digital caliper was used to measure the diameter during extrusion and the target value was 1.75 mm.

Table 1 - HME formulations

Formulation	CBD (%)	PEO (%)	EPO (%)	Ratio PEO/EPO
F1	10	72	18	80/20
F2	10	54	36	60/40
F3	10	45	45	50/50
F4	10	36	54	40/60
F5	10	18	72	20/80

2.4. Design and Printing of the Formulations

Formulations F1 to F5 were printed into cylinder referred as P2 on Fig. 1. The formulation which allowed the greatest increase of CBD apparent aqueous solubility was then printed using the six design templates in order to evaluate which properties were influenced by the morphology of the printed forms. The six designs of oral forms were created online using TinkerCAD (https://tinkercad.com/) for the cylindrical shapes and Shapeways (https://shapeways.com/) for the gyroidal shapes (Fig. 1). The term gyroid has been chosen to describe the capsule-like shapes with or without villi. The three gyroids have 100% of infill because P4 is a solid form and the villi of P5 and P6 are not inside the printed form. The obtained .stl files were converted to gcode files using the software Ultimaker Cura, version 4.11.0 (Ultimaker, The Netherlands).

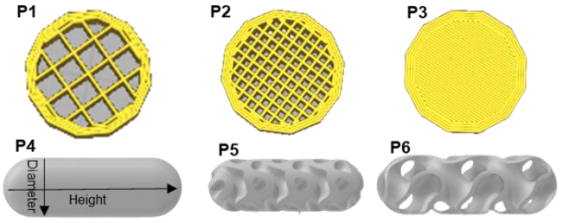

Formulation	Diameter (mm)	Height (mm)	Infill (%)
P1	15	6.20	20
P2	15	4.35	50
P3	15	3.68	100
P4	6.4	25	100
P5	8	25	100
P6	8.2	25	100

Figure 1 - Representation of the six designs (left) and theoretical morphological characteristics and % of infill for each design (right).

The dimensions of each design were adjusted in order to achieve a target mass of 650 mg per printed form which corresponds to an equivalent of 65 mg of CBD. This dosage was chosen in order to be within the dose range tested in the different studies found in the literature [7]. The printed forms were produced with a 3D Original Prusa i3 MK3 printer (Prusa, Prague, Czech Republic) equipped with a 0.4 mm nozzle. As the melted formulations were sticky, a heating-resistant scotch tape was placed on it in order to remove the product easily from the heated platform. The printing temperature and bed temperature were set at 180 °C and 25 °C, respectively. The printing speed was 40 mm/s for the cylinders and 28 mm/s for the gyroids.

2.5. X-ray Diffraction

In order to evaluate the physical state of CBD once printed, disks (23.12 mm diameter x 1.00 mm height) made of drug loaded mixtures of Eudragit®EPO and Polyox®N10 were printed and analyzed. X-ray diffractograms were collected using a Bruker D8 TWIN-TWIN diffractometer in Bragg-Brentano configuration (Cu Kalpha radiation, variable divergence slit V6, sample rotation 15 rpm) with a Lynxeye XET detector in 1D mode (192 channels) and a total scan time of 15 or 30 min for a 0.02° step size.

2.6. Drug Content of Filaments and Printed Forms

Since the formulations are exposed to high temperatures during both stages of their production, the drug content was measured after the HME and after the printing steps. Samples of 20-30 mg were cut from the filaments and the printed forms and dissolved in acetonitrile prior to HPLC analysis. A validated reverse phase high-performance liquid chromatography (HPLC) analytical method, described in a previous work, was used [30]. The HPLC equipment consisted of an Agilent® 1100 (Santa Clara, USA) with OpenLab CDS lC ChemStation version C.01.05 as the software. The mobile phase was composed of water/acetonitrile (38/62% (v/v)) and the column was Zorbax® C18 300 SB with particles of 3.5 µm (150 mm x 4.6 mm ID). The flow rate was set at 1.0 mL/min and the temperature was kept at 30 °C. The injection volume was 20.0 µL, the chromatographic run time was 10 min, CBD retention time was 5.9 min and the detection of CBD was made at a wavelength of 240 nm. The measurements were carried out in triplicate.

2.7. Computerized Tomography Scan

In order to measure their volume and surface area (SA), the printed forms were analyzed with a computerized tomography scan, Skyscan 1172/G (Bruker, Billerica, Massachusetts, United States). The voltage of the x-ray source was 100 kV, and a 0.5 mm aluminum filter was used to harden the x-rays (RX). The magnification was set for a pixel size of 19.91 µm, taking into account 4x4 binning at the detector. The exposure time of an x-ray was 300 ms, for a total of 1,200 360° radios per acquisition. Reconstruction was performed on NRecon software (v. 1.7.3.1), using ring artifact correction (level 5) and 20% beam hardening correction. The processing was carried out on the Avizo software (v. 9.2) supplemented with calculation modules and scripts which were coded. The reconstructions first went through a median filter using an 18-neighborhood, then a thresholding was performed (threshold identified by the Otsu method). The larger 6-connected component has been extracted, and the cavities (all 26-connected components of the background except the largest) have been plugged. The technique of marching cubes was used to triangulate the interface of the solid with the exterior, then a Gaussian smoothing (2 iterations with a lambda of 0.6) was applied before measuring the area.

2.8. Characterization of the Printed Forms Properties

As there is no monograph dedicated to the printed products yet, they were characterized with tests based on the monograph dedicated to the uncoated tablets of the European Pharmacopeia Edition 11.2.

Friability Test

Ten printed forms of each design were randomly taken and friability test was conducted using a Friabilator USP F2 Sotax® (Aesch, Switzerland) according to the monograph 2.9.7. Eur. Ph. Edition 11.2.

Tensile Strength (TS)

The tensile strength of each designed printed forms was determined in triplicate using the breaking force (F) measured by a crushing strength tester Pharmatron MT-50 Sotax® (Aesch, Switzerland) and with the following equations [31]:

$TS = \frac{2F}{\Pi D t}$ for cylinders

$TS = \frac{2}{3}\left(\frac{10F}{\Pi D^2\left(2.84\frac{t}{D} - 0.126\frac{t}{W} + 3.15\frac{W}{D} + 0.01\right)}\right)$ for gyroids

Where:

D is the diameter
t is the overall thickness
W is the wall height

The measure of the tensile strength was preferred to the simple measurement of the hardness, described in the tablet monograph, in order to normalize the hardness according to the shape of the printed form.

Mass Variation

Ten printed forms of each design were individually weighted and the Acceptance Value (AV) was calculated according to the monograph 2.9.40. Eur. Ph. Edition 11.2.

Uniformity of Mass

Ten printed forms of each design were weighed and the average mass was determined according to the monograph 2.9.5 Eur. Ph. Edition 11.2.

In Vitro Drug Release Studies

The dissolution tests were carried out using the USPII paddle method apparatus AT7 (Sotax®, Switzerland). The first set of dissolution tests involved formulations containing different EPO/PEO ratios in a cylinder shape with 50% infill (P2), while the second set

involved the best formulation printed in six different shapes (P1-P6). Crystalline CBD filled into capsules and the printed formulations were weighed down and placed in a dissolution vessel containing 500 mL of HCl 0.1 M. The stirring speed was 100 rpm and the temperature was maintained at 37 °C during 4h. Aliquot samples of 2.0 mL were withdrawn at 5, 15, 30, 45, 60, 90, 120, 180 and 240 min. An equal volume of fresh dissolution medium was replaced after each withdrawal. Samples were then analyzed by HPLC. The dissolution tests were carried out in triplicates.

2.9. Statistical Analysis

One-way ANOVA with a Tukey post-test was used thanks to GraphPad Prism 5.0 software to analyze the results. Differences in results were considered significant with *$p \leq 0.05$ and ** $p \leq 0.01$.

3. Results and discussion

3.1. Impact of the Polymers Ratio on the Dissolution Speed

3.1.1. Filaments extrusion and Printed Forms Production

The filament diameter is a crucial parameter to control before the printing. Indeed, it influences the traction of the filament by the two driving wheels of the printer as well as the mass and the dimensions of the final printed form. Achieving an accurate and consistent filament diameter is challenging and the production process of this filament sometimes needs to be modified. For example, the temperature, feed rate or screw speed can be changed to vary the diameter of the filament [32]. Extra equipment can also be added to the process, such as the use of a filament maker which is composed of an extruder that melts the material and extrudes it through a die, producing a filament that is pulled around a spool [33]. An optical sensor allows a very precise adjustment of the filament diameter. In this work, the diameter of the extruded filaments of F1, F2, F3, F4 and F5 measured at 20 different sections, was relatively constant with a range between 1.69 and 1.80 mm. This proved the suitability of the melt pump with the addition of a conveyor belt to precisely control the diameter.

Another essential parameter to obtain a printable formulation is the flexibility of the filament. EPO was chosen as a polymeric matrix for the increase of the apparent aqueous solubility, in an acid medium, of CBD following a previous study [16]. Due to its ability to dissolve rapidly in the stomach, EPO is suitable for the production of IR formulations [34]. However, its brittleness makes it not printable without being plasticized so it was mixed with PEO for the production of the filaments [35]. Indeed, too brittle filaments could break between the two gears of the printer. PEO has already demonstrated its ability to increase the printability of EPO by plasticizing it [36]. All the formulations could be extruded, with a torque decreasing proportionally with the increase in the proportion of PEO, highlighting its plasticizing effect [37]. The resulting filaments were smooth, translucent, suggesting a complete dissolution of CBD in the polymers blend, and slightly yellow, due to the natural color of CBD [38].

Moreover, all the formulations could be printed, even those containing large proportions of EPO confirming the increase in flexibility of this polymer, even with low percentages of PEO.

3.1.2. Drug Recovery

The HME and the FDM processes both involving relatively high temperatures thus the drug recovery was evaluated after HME and after the 3D printing of the five formulations (F1-F5). Since the final forms produced by FDM 3D printing are intended for hospital or public pharmacies whereas the filament will be produced as a raw material, the limits of the CBD content have been set between 90 and 110% for printed forms and 95-105% for the filaments.

The results on Figure 2 show that the drug recovery, whether in the filaments or in the printed form, was between the defined limits, with a minimum and maximum of 98.5±0.5% and 102.5±0.7%, respectively. Moreover, there were no significant differences before and after the printing, for each formulation. These results are in accordance with the TGA analysis (appendix), as the extrusion and printing temperatures (140 °C and 180 °C, respectively) did not exceed the degradation temperature of the CBD (220 °C).

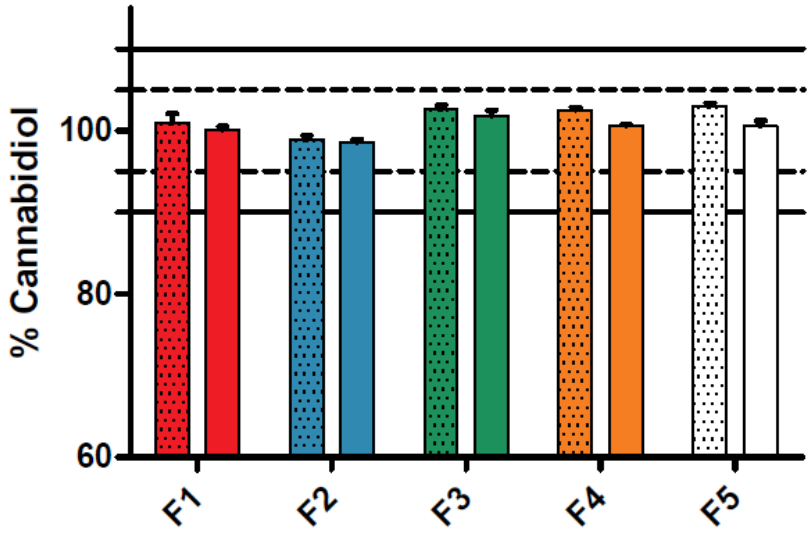

Figure 2 – CBD recovery of the filaments (dashed columns) and the printed forms (empty columns) of F1, F2, F3, F4 and F5. The defined limits of the drug recovery in the filaments are represented by the dotted lines at 95 and 105% and by the continuous lines at 90 and 110% for the drug recovery in the printed forms.

3.1.3. In Vitro Dissolution Tests

The dissolution in an acidic medium of formulations F1, F2, F3, F4 and F5 was first carried out in order to choose the formulation which allowed the fastest dissolution of CBD. The curves on Figure 3.a show that each formulation improved the apparent aqueous solubility of CBD compared to raw CBD. This improvement is explained first by the maintenance of the CBD in its amorphous form by the two polymers in the printed forms, confirmed by the absence of the characteristic peaks of the crystalline CBD around 10° on the diffractogram patterns of F1, F2, F3, F4 and F5 printed disks (Fig.4). The apparent solubility of the CBD is also improved by the property of EPO to create micelles which can solubilize poor water-soluble molecules [39]. However regarding the dissolution rate, only F5 conducted to an IR of the CBD, with 83.91 ± 2.15% dissolved after 30 min which is significantly different from the other four formulations (Fig. 3.b). Indeed, F1, F2, F3 and F4 respectively dissolve 54.03 ± 4.64%, 58.85 ± 8.57%, 59.69 ± 1.92% and 65.85 ± 9.19%. This could be explained by the property of EPO to substantially solubilize drugs in acidic solution [40]. These differences in dissolution rates could also be explained by the PEO/EPO ratio. PEO is well-known to form, on

contact with aqueous media, a hydrogel which can slow the liberation of the drug [34,41]. This gelling effect leads to the conclusion that the more PEO there is, the slower the CBD will dissolve.

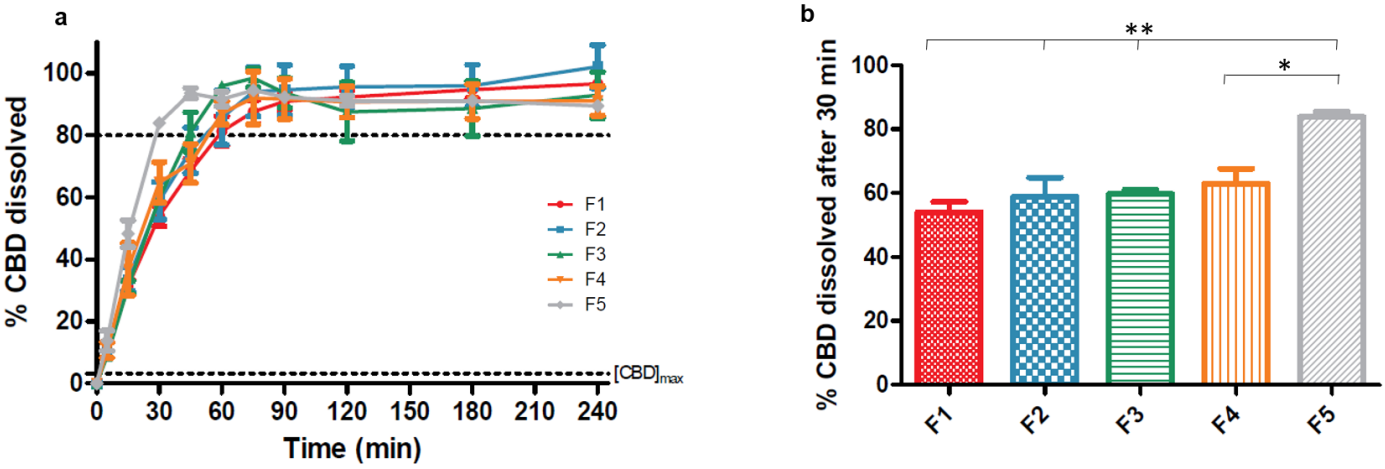

*Figure 3 – Dissolution profile of F1 (red), F2 (blue), F3 (green), F4 (orange) and F5 (gray) in HCl 0.1 M, with the lower dashed line representing the solubility at saturation of the raw CBD in the dissolution medium and the upper dashed line representing the 80% of dissolved CBD (a) and focus on the percentage of dissolved CBD after 30 min depending on the Eudragit®EPO/Polyox®N10 ratio with * representing p value ≤ 0.05 and ** representing p value ≤ 0.01 (b).*

The formulation F5 (PEO/EPO (20/80)) was selected to study the pharmaceutical quality of the six designs of printed forms due to its ability to immediately release the CBD.

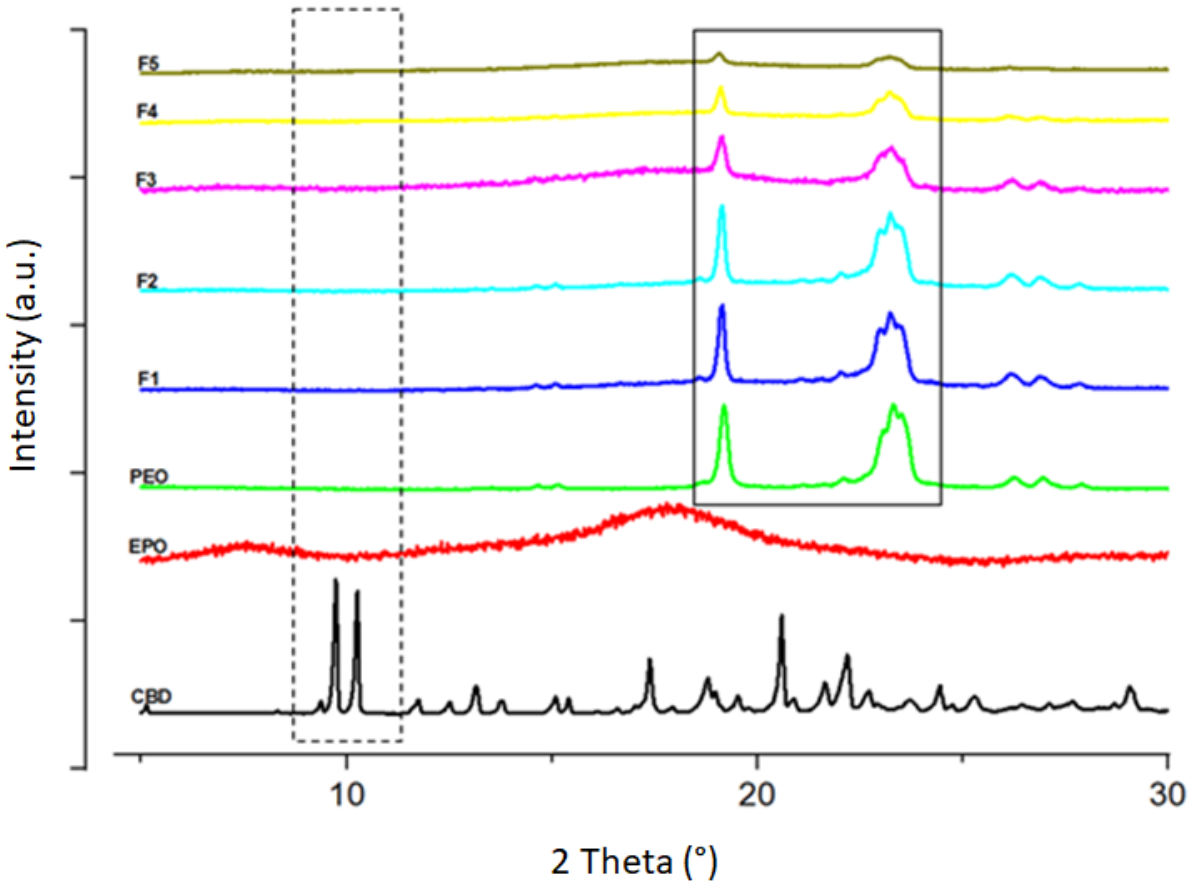

Figure 4 - XRD patterns of crystalline CBD (black), raw EPO (red), raw PEO (light green) and the printed disks composed of F1 (dark blue), F2 (light blue), F3 (purple), F4 (yellow) and F5 dark green). The diffractogram of EPO shows a halo confirming the amorphous state of this polymer. The dotted frame shows the absence of the characteristic peaks of crystalline CBD at about 10° in each formulation, which means that CBD is completely amorphous in all printed disks. The continuous line frame highlights the semi-crystalline character of PEO which shows characteristic peaks at about 19° and 24°. These peaks are also present in the printed disks, suggesting rapid recrystallization of PEO.

3.2. Impact of the morphology on the reproducibility and quality

Cylinders and capsule-like forms (called gyroid in this study) are the most used shapes for the production of drugs. In that regard, these shapes were chosen to study the impact of the morphology on the reproducibility of the printed forms manufacture, their mechanical properties and their *in vitro* dissolution performance.

Each design could be printed by the printer, but with different durations (Fig.6 and Table 2). Indeed, the cylinders were printed about three times faster than gyroids. It could be explained by the more complex structure of the gyroids compared to the one of the cylinders. One of the ways to print complex shapes accurately is to reduce the printing speed [42].

The diameter and height of the 10 printed forms of each design were measured and the deviation from the dimensions of the digital model is shown in Table 2. All the printed forms had a deviation of the diameter from -1 ± 0.15% to 1 ± 0.51% compared to the digital model.

Regarding the height, the printed forms had a deviation ranging from -1.44 ± 0.23% to -0.33 ± 0.71%. These narrow ranges are similar to other studies [43,44].

As described above, the mass of the printed product depends on the uniformity of the diameter of the filament fed into the printer. The *mass variation* and *uniformity of mass* tests ensure that the mass of all the printed forms produced is within the limits defined by the European Pharmacopeia. Figure 7 represents the mean mass measured on ten printed forms of each design and the acceptance value for each design. Results show a deviation of the mass of the printed forms compared to the target mass (650 mg) going from -18.43 mg for P5 to +24.99 mg for P1. Numerous ranges of mass deviation from the mass target are found in the literature [45,46]. The deviation from this study is among the largest. This can be explained by the relatively large size of the printed forms. Indeed, the mass of the printed shapes is mainly influenced by the consistency of the diameter of the previously extruded filament. The larger the printed forms, the more the inconsistency of the filament will be reflected in the mass deviation. Concerning the mass uniformity, the acceptance values of P4, P5 and P6 (gyroids) tend to be higher than the ones of P1, P2 and P3 (cylinders). This is probably another consequence of the complexity of the gyroid structure. However, all the designs were in accordance with the mass variation test, as every acceptance value was below 15.00, and with mass uniformity test, as deviations of respectively -7.69% and +6.36% for the most under and over weighted printed forms were observed. Moreover, no more than two printed forms per formulation deviated from more than 5% of the average mass. The test was therefore compliant and proved the ability of the FDM to produce printed forms with adequate reproducibility.

The results concerning the printed forms dimensions and the mass variation and uniformity highlight the good reproducibility of the printed forms manufacture by the 3D Original Prusa i3 MK3 printer, no matter the design to print.

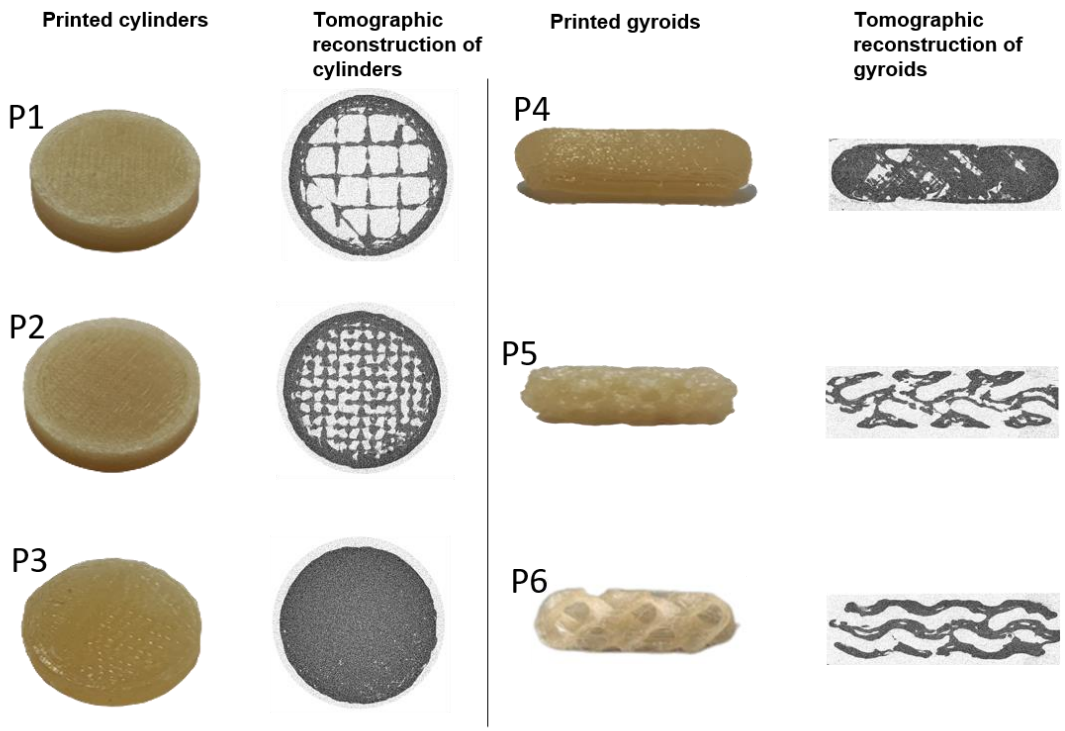

410

411 *Figure 6 - Pictures of the printed forms and their respective tomographic reconstruction performed by*
412 *Computerized Tomography Scan.*

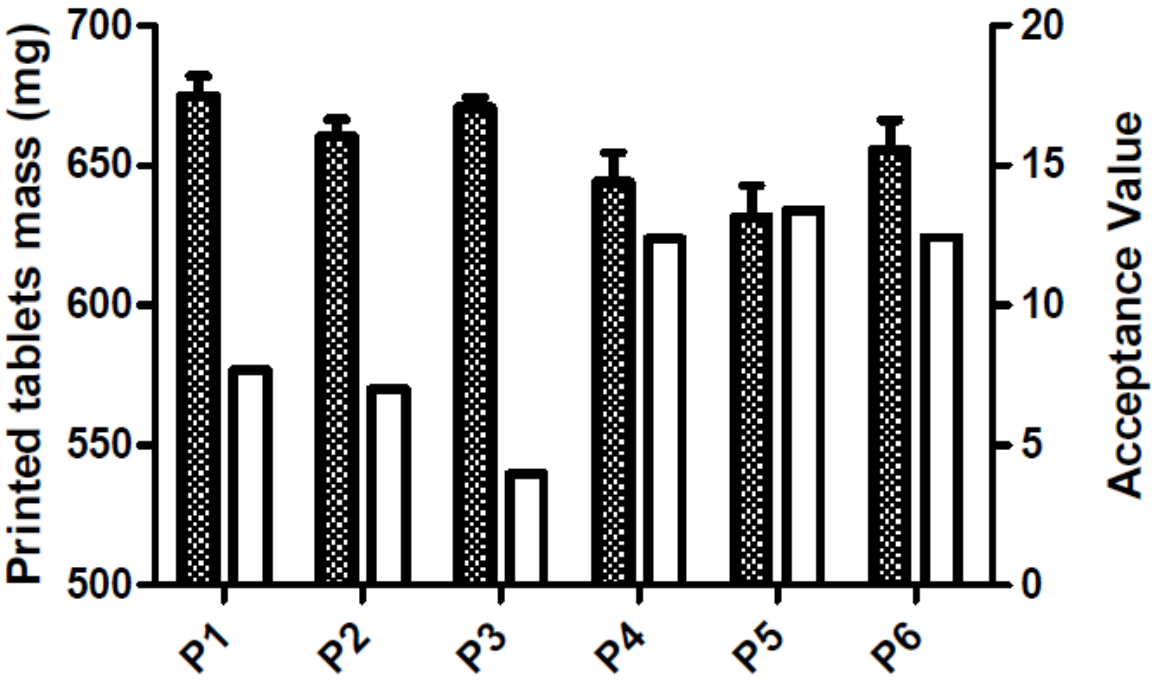

413

414 *Figure 7 - Mass of the printed form of the 6 designs (mean and SD, n = 10) represented by the dashed columns*
415 *and the acceptance value for each design represented by the empty columns (measured on ten printed forms).*

416

417 In addition to the reproducibility, the morphology of the final printed form influences its
418 mechanical properties [47,48]. The *friability* and the *tensile strength* are two important
419 parameters concerning the study of the integrity of oral solid dosage forms during the

production, transport and handling by the patient. The results on Table 2 show that the mass loss during the friability test was <1% for each formulation and met the Eur. Ph. recommendation. Compared to the standard techniques for the manufacturing of oral solid forms such as tableting, or other 3D printing techniques like powder-based 3D printing, FDM allows the production of products with a poor friability without additional steps or excipients (Chang et al., 2021; Infanger et al., 2019; Lakshman et al., 2011).

Table 2 - Characterization of the printed forms

	Diameter[a] (%) (n=10)	Height[a] (%) (n=10)	Surface Area (mm²)	SA/V ratio	Friability (%)*	Tensile Strength (MPa) (n=3)	Printing Time (min)
P1	99.00±0.15	99.67±0.71	1129.1	1.86	0.25	1.80±0.01	≈ 5
P2	100.53±0.13	99.54±0.09	908.3	1.53	0.11	2.43±0.04	≈ 5
P3	101.00±0.17	98.91±0.17	792.8	1.34	0.24	4.32±0.27	≈ 5
P4	100.47±0.14	98.56±0.16	626.6	1.03	0.14	4.63±0.07	≈ 14
P5	101.00±0.51	98.72±0.34	2528.8	4.09	0.21	0.58±0.01	≈ 14
P6	99.39±0.17	98.56±0.23	2914.6	4.83	0.85	0.25±0.02	≈ 14

a% = printed model/digital model (measured in triplicate). * = measured on ten printed forms.

Finally, dissolution tests were conducted to study the impact of the morphology on the release of the CBD in HCl 0.1 M. Fig. 8.b shows that the dissolution profiles during the first 45 min of the test are different. Every printed form allowed an IR of CBD (>80%), but at different dissolution rates. The differences between the dissolution rates can be explained by the SA/V ratio of the printed forms (Table 2). The higher this ratio, the faster the dissolution, confirmed by Fig. 8.d which shows the time to reach 80% of CBD dissolved from the printed forms in function of their SA/V ratio [43,49]. Indeed, the greater the SA/V, the less time it takes to dissolve 80% of the CBD.

P5 and P6 even exceeded 80% dissolution of CBD in less than 15 min which is equivalent to more than 52 mg of CBD. This is, to the best of our knowledge, the dissolution of the highest dose of a poor soluble API from a printed form at this time. Indeed, formulations manufactured by FDM show generally a slower release than the ones manufactures by conventional techniques [50]. This may be caused by the rigid structures formed after the successive melting and solidification by cooling of the polymeric product conducting to a slow erosion-based dissolution of the product. Alhijjaj *et al.* investigated the polymeric blend of EPO/polysorbate 80/polyethylene glycol 4000/PEO to print IR formulations of felodipin [51]. The immediate release was obtained as 84.3% of the drug dissolved in 30 min, but it represents only about 5 mg of the drug. Similarly, Sadia *et al.* printed blends of EPO/triethylcitrate/tri-calcium phosphate/drug using four different drugs including the poorly water-soluble prednisolone [35]. The *in vitro* dissolution tests showed 85% of dissolved drug in 30 min, equal to about 25 mg of

prednisolone. In a more recent study, Crisan *et al.* aimed at printing IR forms containing high doses of diclofenac sodium. They managed to release up to about 70 mg of API in 10 min in a pH 6.8 buffer. However, even is diclofenac sodium is classified in BCS II in acidic media, it is highly soluble in this pH 6.8 buffer [52,53].

The dissolution tests showed that, for a constant weight, the gyroids allow a faster dissolution of the CBD as these designs had a higher SA/V ratio. However, the shape of the printed forms had no influence on the upkeep of the CBD concentration during the dissolution test once the maximum of dissolution was achieved. Indeed, supersaturated solutions are subject to drug precipitation, especially if the drug is released rapidly [55]. However, Figure 8.c shows an upkeep of the CBD concentration once the maximum of dissolution was achieved, for four hours, no matter the time required to reach this maximum, and therefore no matter the shape.

The data of the dissolution tests conducted in this study show that FDM 3D printing allows the manufacturing of oral solid dosage forms with adjustable dissolution speed and rate, which is very interesting for drugs with different therapeutic uses such as CBD.

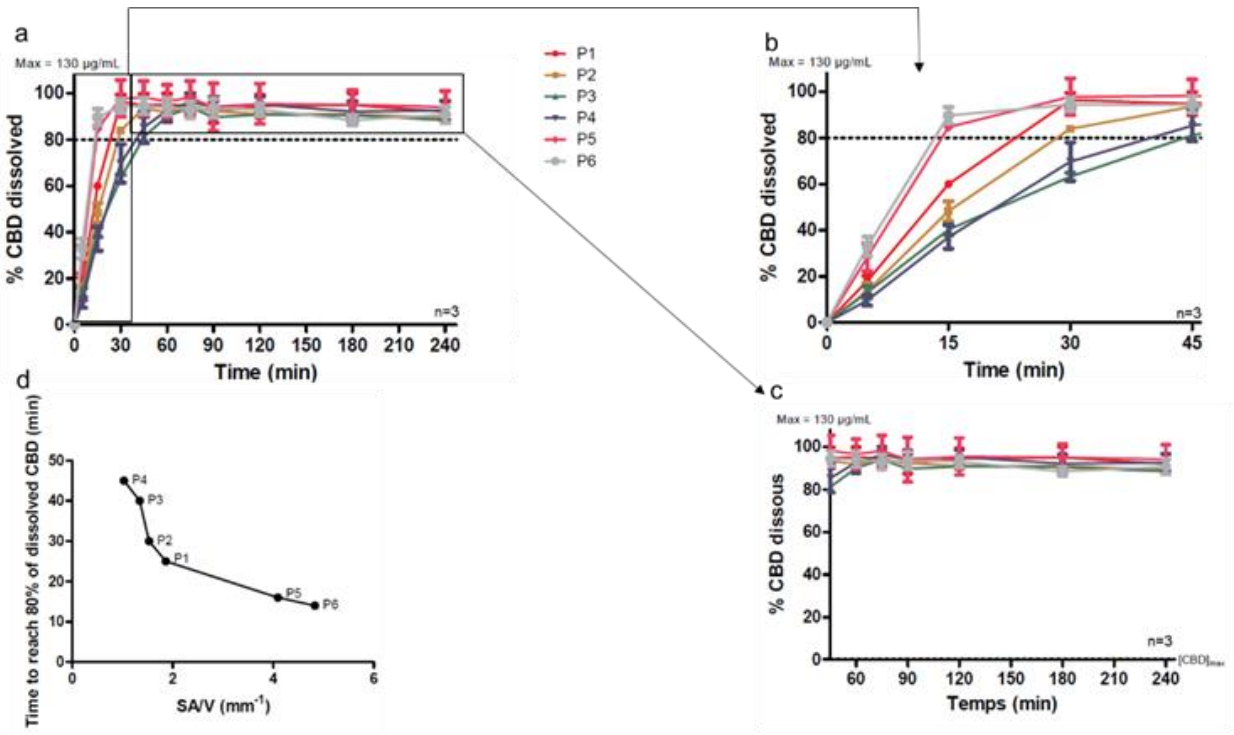

Figure 8 – Dissolution profile of P1 (red), P2 (yellow), P3 (green), P4 (blue), P5 (pink) and P6 (gray) during the whole test (a), between the beginning and 45 min of the test (b) and between 45 and the end of the test (c) and the time to reach 80% of dissolved CBD from the printed forms as a function of the SA/V ratio.

Among the printed forms that allow an IR of CBD (P1, P2, P5 and P6), even if P5 and P6 achieve 80% release significantly faster than the others (P value ≤ 0.01), P1 was chosen for the rest of the study because its production is three times faster than P5 and P6.

3.3. Evaluation of the dosage adaptability

This section was intended to support the hypothesis that by manufacturing printed forms with the same shape and infill but with different dosages, the requirements of the Eur. Ph. and the reproducibility described above would still be fullfilled. The dimensions of cylinders with 20% infill based on the design of P1 were adjusted to obtain printed forms containing 32.5 or 97.5 mg of CBD which are 50% and 150% of the target dosage of P1, respectively. The characterstics of the printed cylinders with different dosages have been compiled in Table 3. The deviation of the diameter of cylinders containing 32.5 mg and 97.5 mg of CBD from the digital model are similar to those encountered by the cylinder containing 65 mg of CBD with a deviation of -0.3±0.05% and -1.88±0.2%, respectively. The same goes for the height, with a deviation of +0.04±0.17% for the cylinders containing 32.5 mg of CBD and -1.98±0.31% for the cylinders with 97.5 mg of CBD, compared to the digital model. The deviation of the average mass of the printed forms compared to the target mass was smaller for the cylinders with 32.5 mg of CBD (+7.20 mg) than for the cylinders with 97.5 mg of CBD (-30.02 mg). This could be due to the proportional effect of the inconstancy of the filament diameter and the size of the printed shape, as explained above. However, both dosages allowed a mass uniformity in accordance with the Eur. Ph., as the acceptance values were below 15.00.

No significant changes were expected in the mechanical properties by modifying the printed forms dimensions and dosage as the manufacturing process remains the same. Friability test compliance was unaffected by these changes, confirming the rigid structure of the printed shapes. It goes the same for the tensile strength which was not affected as it is normalized according to the shape of the printed form.

Table 3 - Characterization of the printed cylinders with 20% infill and different dosages

Dosage (mg CBD)	Diameter [a] (%) n=10	Height[a] (%) n=10	Deviation of average mass (mg)*	SA/V ratio	Friability (%)*	Acceptance Value*	Tensile Strength (MPa) n=10	Printing Time (min)
32.5	99.70±0.05	100.04±0.17	+7.20±1.77	1.36	0.21	3.11	2.13± 0.07	≈ 3
65	99.00±0.15	99.67±0.71	+24.99±3.05	1.86	0.25	7.69	1.80± 0.01	≈ 5
97.5	98.12±0.20	98.02±0.31	-30.02±2.87	0.98	0.26	14.53	2.00± 0.2	≈ 7

a% = printed model/digital model (measured in triplicate). * = measured on ten printed forms.

The dissolution tests performed with the three dosages showed a dissolution rate proportionnal to the dosage of CBD at the start of the test (Fig. 9). Indeed, the 32.5 mg, 65 mg and 97.5 mg cylinders dissolved 43.93±2.01%, 59.98±0.29% and 77.48±3.63% after 15 min, respectively. However, after 30 min of dissolution testing, the three dosage

forms reached their maximum of dissolution which was maintained until the end of the test. More than 80% of CBD was dissolved for the three formulations, translating an IR.

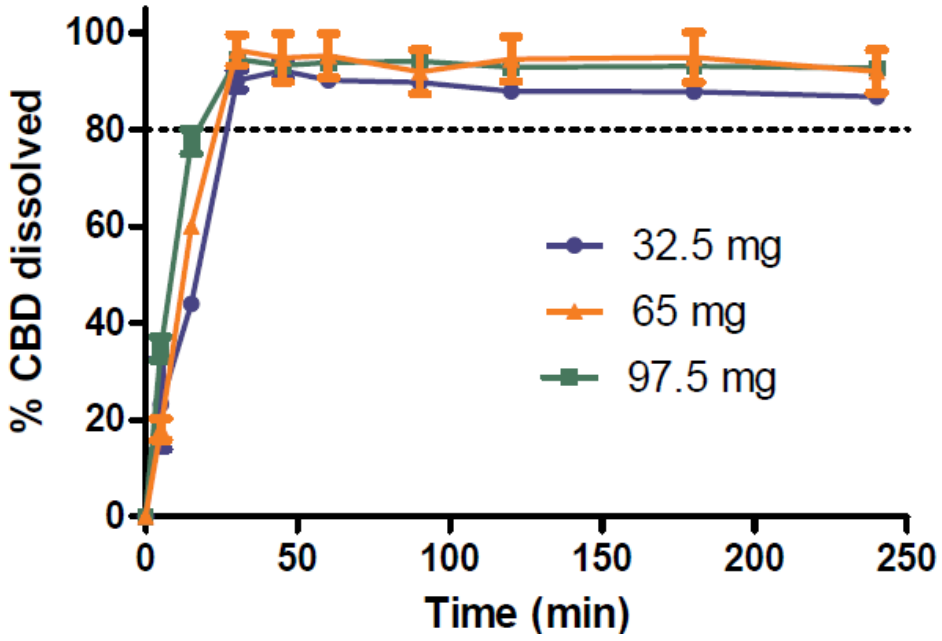

Figure 9 - Dissolution profile of the printed cylinders with 20% infill and different dosages.

These results concerning the dosage adaptability show the advantage of using FDM for the production of solid oral forms containing APIs used at various dosages depending on the treatment. Indeed, the dosage could be customized, by the simple step of modifying the digital pattern intented to be printed, without affecting the quality of the final product.

4. Conclusion

The pharmaceutical industry is paying more and more attention to personalized medicine. This study has proven that challenges inherent to the manufacture of customized dosage forms can be overcome by fused deposition modeling 3D printing. Indeed, printed forms of cannabidiol with complex structures were successfully produced with a good reproducibility. Different dissolution rates of cannabidiol were obtained from these printed forms, even with a high quantity of cannabidiol. Since there are no specific guidelines for the product manufactured by 3D printing, the quality control of these printed forms was conducted following the monograph concerning the uncoated tablets of the European Pharmacopoeia, as recommended by the Food and Drug Administration. As a result, all printed forms were in accordance with the specifications of this monograph. In addition, the modification of the strength of these printed forms had no impact of their quality. These results are encouraging when it comes to the implementation of FDM in hospitals or public pharmacies in order to develop personalized medicine affordable by every patient.

5. Acknowledgments

The authors wish to acknowledge FEDER funds for the support in SOLPHARE FEDER project (884148-329407) and the Fonds Léon Fredericq for the support in project 2021-2022-12. The authors also wish to thank Wenda Lazzari and Astrid Couturier (Mithra CDMO) for the loan and the support of the melt pump.

6. References

[1] M. Ryan, Cannabidiol in epilepsy: The indications and beyond, Ment. Heal. Clin. 10 (2020) 317–325. https://doi.org/10.9740/mhc.2020.11.317.

[2] M. Mazurkiewicz-Bełdzińska, M. Zawadzka, Use of cannabidiol in the treatment of epilepsy, Neurol. Neurochir. Pol. 56 (2022) 14–20. https://doi.org/10.5603/PJNNS.a2022.0020.

[3] M.M. Bergamaschi, R. Helena Costa Queiroz, M. Hortes, N. Chagas, D. Chaves Gomes De Oliveira, B.S. De Martinis, F. Kapczinski, J. Quevedo, R. Roesler, N. Schrö Der, A.E. Nardi, R. Martín-Santos, J.E.C. Hallak, A.W. Zuardi, J. Alexandre, S. Crippa, Cannabidiol Reduces the Anxiety Induced by Simulated Public Speaking in Treatment-Naı¨veNaı¨ve Social Phobia Patients, Neuropsychopharmacology. 36 (2011) 1219–1226. https://doi.org/10.1038/npp.2011.6.

[4] C.G. Heider, S.A. Itenberg, J. Rao, H. Ma, X. Wu, Mechanisms of Cannabidiol (CBD) in Cancer Treatment: A Review, (2022). https://doi.org/10.3390/biology11060817.

[5] P. McGuire, P. Robson, W.J. Cubala, D. Vasile, P.D. Morrison, R. Barron, A. Taylor, S. Wright, Cannabidiol (CBD) as an adjunctive therapy in schizophrenia: A multicenter randomized controlled trial, Am. J. Psychiatry. 175 (2018) 225–231. https://doi.org/10.1176/appi.ajp.2017.17030325.

[6] Y.L. Hurd, S. Spriggs, J. Alishayev, G. Winkel, K. Gurgov, C. Kudrich, A.M. Oprescu, E. Salsitz, Cannabidiol for the Reduction of Cue-Induced Craving and Anxiety in Drug-Abstinent Individuals With Heroin Use Disorder: A Double-Blind Randomized Placebo-Controlled Trial, Am J Psychiatry. 176 (2019) 911–922. https://doi.org/10.1176/appi.ajp.2019.18101191.

[7] S. Millar, N. Stone, Z. Bellman, A. Yates, T. England, C.A. Sophie Millar, A systematic review of cannabidiol dosing in clinical populations, Artelo Biosci. Biotechnol. Biol. Sci. Res. Counc. (2019). https://doi.org/10.1111/bcp.14038.

[8] O.M. Feeney, M.F. Crum, C.L. McEvoy, N.L. Trevaskis, H.D. Williams, C.W. Pouton, W.N. Charman, C.A.S. Bergström, C.J.H. Porter, 50 years of oral lipid-based formulations: Provenance, progress and future perspectives, Adv. Drug Deliv. Rev. 101 (2016) 167–194. https://doi.org/10.1016/j.addr.2016.04.007.

[9] Y. Nakano, M. Tajima, E. Sugiyama, V.H. Sato, H. Sato, Development of a Novel Nano-emulsion Formulation to Improve Intestinal Absorption of Cannabidiol, Med. Cannabis Cannabinoids. 2 (2019) 35–42. https://doi.org/10.1159/000497361.

[10] N.N.B. Williams, T.R. Ewell, K.S.S. Abbotts, K.J. Harms, K.A. Woelfel, G.P. Dooley, T.L. Weir, C. Bell, Comparison of five oral cannabidiol preparations in adult humans: Pharmacokinetics, body composition, and heart rate variability, Pharmaceuticals. 14 (2021) 1–14. https://doi.org/10.3390/ph14010035.

[11] J.M. Hobbs, A.R. Vazquez, N.D. Remijan, R.E. Trotter, T. V McMillan, K.E. Freedman, Y. Wei, K.A. Woelfel, O.R. Arnold, L.M. Wolfe, S.A. Johnson, T.L. Weir, C.A. Sarah Johnson, Evaluation of pharmacokinetics and acute anti-inflammatory potential of two oral cannabidiol preparations in healthy adults, (2020). https://doi.org/10.1002/ptr.6651.

[12] K.F. Boehnke, · Winfried Häuser, M.-A. Fitzcharles, Cannabidiol (CBD) in Rheumatic Diseases (Musculoskeletal Pain), Curr. Rheumatol. Rep. 24 (2022) 238–246. https://doi.org/10.1007/s11926-022-01077-3.

[13] B.N. Tran, Q. Van Pham, B.T. Tran, G. Thien Le, A.H. Dao, T.H. Tran, C.N. Nguyen, Supercritical CO2 impregnation approach for enhancing dissolution of fenofibrate by adsorption onto high-surface area carriers, J. Supercrit. Fluids. 184 (2022) 105584. https://doi.org/10.1016/j.supflu.2022.105584.

[14] J. Petitprez, · François-Xavier Legrand, · Catherine Tams, · J D Pipkin, V. Antle, M. Kfoury, S. Fourmentin, Huge solubility increase of poorly water-soluble pharmaceuticals by sulfobutylether-β-cyclodextrin complexation in a low-melting mixture, Environ. Chem. Lett. 20 (2022) 1561–1568. https://doi.org/10.1007/s10311-022-01415-y.

[15] A. Singh, G. Van den Mooter, Spray drying formulation of amorphous solid dispersions, Adv. Drug Deliv. Rev. 100 (2016) 27–50. https://doi.org/10.1016/j.addr.2015.12.010.

[16] O. Jennotte, N. Koch, A. Lechanteur, B. Evrard, Development of amorphous solid dispersions of cannabidiol: Influence of the carrier, the hot-melt extrusion parameters and the use of a crystallization inhibitor, J. Drug Deliv. Sci. Technol. 71 (2022) 103372. https://doi.org/10.1016/j.jddst.2022.103372.

[17] I. Koutsamanis, M. Spoerk, F. Arbeiter, S. Eder, E. Roblegg, Development of Porous Polyurethane Implants Manufactured via Hot-Melt Extrusion, Polymers (Basel). 12 (2020). https://doi.org/10.3390/polym12122950.

[18] A. Butreddy, S. Sarabu, S. Bandari, A. Batra, K. Lawal, N.N. Chen, V. Bi, T. Durig, M.A. Repka, Influence of Plasdone ™ S630 Ultra-an Improved Copovidone on the Processability and Oxidative Degradation of Quetiapine Fumarate Amorphous Solid Dispersions Prepared via Hot-Melt Extrusion Technique, AAPS PharmSciTech. 22 (2021) 196. https://doi.org/10.1208/s12249-021-02069-9.

[19] N.N. Mohammed, S. Majumdar, A. Singh, W. Deng, N.S. Murthy, E. Pinto, D. Tewari, T. Durig, M.A. Repka, Klucel™ EF and ELF polymers for immediate-release oral dosage forms prepared by melt extrusion technology, AAPS PharmSciTech. 13 (2012) 1158–1169. https://doi.org/10.1208/s12249-012-9834-z.

[20] N. Dumpa, A. Butreddy, H. Wang, N. Komanduri, S. Bandari, M.A. Repka, 3D printing in personalized drug delivery: An overview of hot-melt extrusion-based fused deposition modeling, Int. J. Pharm. 600 (2021) 120501. https://doi.org/10.1016/j.ijpharm.2021.120501.

[21] N. Samiei, Recent trends on applications of 3D printing technology on the design and manufacture of pharmaceutical oral formulation: a mini review, Beni-Suef Univ. J. Basic Appl. Sci. 9 (2020). https://doi.org/10.1186/s43088-020-00040-4.

[22] J. Quodbach, M. Bogdahn, J. Breitkreutz, R. Chamberlain, K. Eggenreich, A.G. Elia, N. Gottschalk, G. Gunkel-Grabole, L. Hoffmann, D. Kapote, T. Kipping, S. Klinken, F. Loose, T. Marquetant, H. Windolf, S. Geißler, T. Spitz, Quality of FDM 3D Printed Medicines for Pediatrics: Considerations for Formulation Development, Filament Extrusion, Printing Process and Printer Design, Ther. Innov. Regul. Sci. 56 (2022) 910–928. https://doi.org/10.1007/s43441-021-00354-0.

[23] A. Goyanes, F. Fina, A. Martorana, D. Sedough, S. Gaisford, A.W. Basit, Development of modified release 3D printed tablets (printlets) with pharmaceutical excipients using additive manufacturing, Int. J. Pharm. 527 (2017) 21–30. https://doi.org/10.1016/j.ijpharm.2017.05.021.

[24] M. Sadia, A. Isreb, I. Abbadi, M. Isreb, D. Aziz, A. Selo, P. Timmins, M.A. Alhnan, From 'fixed dose combinations' to 'a dynamic dose combiner': 3D printed bi-layer antihypertensive tablets, Eur. J. Pharm. Sci. 123 (2018) 484–494. https://doi.org/10.1016/j.ejps.2018.07.045.

[25] N. Scoutaris, S.A. Ross, D. Douroumis, 3D Printed B Starmix ^ Drug Loaded Dosage Forms for Paediatric Applications, (2018) 1–11.

[26] A. Maroni, A. Melocchi, F. Parietti, A. Foppoli, L. Zema, A. Gazzaniga, 3D printed multi-compartment capsular devices for two-pulse oral drug delivery, J. Control. Release. 268 (2017) 10–18. https://doi.org/10.1016/j.jconrel.2017.10.008.

[27] S. Mohapatra, R.K. Kar, P.K. Biswal, S. Bindhani, Approaches of 3D printing in current drug delivery, Sensors Int. 3 (2022) 100146. https://doi.org/10.1016/j.sintl.2021.100146.

[28] J. Norman, R.D. Madurawe, C.M.V. Moore, M.A. Khan, A. Khairuzzaman, A new chapter in pharmaceutical manufacturing: 3D-printed drug products, Adv. Drug Deliv. Rev. 108 (2017) 39–50. https://doi.org/10.1016/j.addr.2016.03.001.

[29] D. Izgelov, M. Freidman, A. Hoffman, Investigation of cannabidiol gastro retentive tablets based on regional absorption of cannabinoids in rats, Eur. J. Pharm. Biopharm. 152 (2020) 229–235. https://doi.org/10.1016/j.ejpb.2020.05.010.

[30] N. Koch, O. Jennotte, Y. Gasparrini, F. Vandenbroucke, A. Lechanteur, B. Evrard, Cannabidiol aqueous solubility enhancement: Comparison of three amorphous formulations strategies using different type of polymers, Int. J. Pharm. 589 (2020) 119812. https://doi.org/10.1016/j.ijpharm.2020.119812.

[31] K.G. Pitt, M.G. Heasley, Determination of the tensile strength of elongated tablets, Powder Technol. 238 (2013) 169–175. https://doi.org/10.1016/j.powtec.2011.12.060.

[32] J. Aho, J.P. Bøtker, N. Genina, M. Edinger, L. Arnfast, Roadmap to 3D-Printed Oral

642 Pharmaceutical Dosage Forms : Feedstock Filament Properties and Characterization for Fused
643 Deposition Modeling, J. Pharm. Sci. 108 (2019) 26–35.
644 https://doi.org/10.1016/j.xphs.2018.11.012.

645 [33] C. Parulski, O. Jennotte, A. Lechanteur, B. Evrard, Challenges of fused deposition modeling
646 3D printing in pharmaceutical applications: Where are we now?, Adv. Drug Deliv. Rev. 175
647 (2021). https://doi.org/10.1016/j.addr.2021.05.020.

648 [34] H.E. Gültekin, S. Tort, F. Acartürk, Fabrication of Three Dimensional Printed Tablets in Flexible
649 Doses: A Comprehensive Study from Design to Evaluation, SSRN Electron. J. 74 (2022)
650 103538. https://doi.org/10.2139/ssrn.4028237.

651 [35] M. Sadia, A. So, B. Arafat, A. Isreb, W. Ahmed, Adaptation of pharmaceutical excipients to
652 FDM 3D printing for the fabrication of patient-tailored immediate release tablets, Int. J. Pharm.
653 513 (2016) 659–668. https://doi.org/10.1016/j.ijpharm.2016.09.050.

654 [36] S. Henry, L. De Wever, V. Vanhoorne, T. De Beer, C. Vervaet, Influence of print settings on the
655 critical quality attributes of extrusion-based 3d-printed caplets: A quality-by-design approach,
656 Pharmaceutics. 13 (2021). https://doi.org/10.3390/PHARMACEUTICS13122068.

657 [37] M.M. Crowley, F. Zhang, M.A. Repka, S. Thumma, S.B. Upadhye, S.K. Battu, J.W. McGinity,
658 C. Martin, Pharmaceutical applications of hot-melt extrusion: Part I, Drug Dev. Ind. Pharm. 33
659 (2007) 909–926. https://doi.org/10.1080/03639040701498759.

660 [38] J. Macedo, A. Samaro, V. Vanhoorne, C. Vervaet, J.F. Pinto, Processability of poly(vinyl
661 alcohol) Based Filaments With Paracetamol Prepared by Hot-Melt Extrusion for Additive
662 Manufacturing, J. Pharm. Sci. 109 (2020) 3636–3644.
663 https://doi.org/10.1016/j.xphs.2020.09.016.

664 [39] X. Lin, L. Su, N. Li, Y. Hu, G. Tang, L. Liu, H. Li, Z. Yang, Understanding the mechanism of
665 dissolution enhancement for poorly water-soluble drugs by solid dispersions containing
666 Eudragit® E PO, J. Drug Deliv. Sci. Technol. 48 (2018) 328–337.
667 https://doi.org/10.1016/j.jddst.2018.10.008.

668 [40] X. Lin, L. Su, N. Li, Y. Hu, G. Tang, L. Liu, H. Li, Z. Yang, Understanding the mechanism of
669 dissolution enhancement for poorly water- soluble drugs by solid dispersions containing
670 Eudragit ® E PO, J. Drug Deliv. Sci. Technol. 48 (2018) 328–337.
671 https://doi.org/10.1016/j.jddst.2018.10.008.

672 [41] S. Shojaee, P. Emami, A. Mahmood, Y. Rowaiye, A. Dukulay, W. Kaialy, I. Cumming, A.
673 Nokhodchi, An Investigation on the Effect of Polyethylene Oxide Concentration and Particle
674 Size in Modulating Theophylline Release from Tablet Matrices, AAPS PharmSciTech. 16
675 (2015) 1281–1289. https://doi.org/10.1208/s12249-015-0295-z.

676 [42] T.S. Tamir, G. Xiong, Q. Fang, X. Dong, Z. Shen, F.Y. Wang, A feedback-based print quality
677 improving strategy for FDM 3D printing: an optimal design approach, Int. J. Adv. Manuf.

Technol. 120 (2022) 2777–2791. https://doi.org/10.1007/s00170-021-08332-4.

[43] S. Obeid, M. Madžarević, M. Krkobabić, S. Ibrić, Predicting drug release from diazepam FDM printed tablets using deep learning approach: Influence of process parameters and tablet surface/volume ratio, Int. J. Pharm. 601 (2021). https://doi.org/10.1016/j.ijpharm.2021.120507.

[44] C. Wei, N.G. Solanki, J.M. Vasoya, A. V. Shah, A.T.M. Serajuddin, Development of 3D Printed Tablets by Fused Deposition Modeling Using Polyvinyl Alcohol as Polymeric Matrix for Rapid Drug Release, J. Pharm. Sci. 109 (2020) 1558–1572. https://doi.org/10.1016/j.xphs.2020.01.015.

[45] C. Parulski, E. Gresse, O. Jennotte, A. Felten, E. Ziemons, A. Lechanteur, B. Evrard, Fused deposition modeling 3D printing of solid oral dosage forms containing amorphous solid dispersions: How to elucidate drug dissolution mechanisms through surface spectral analysis techniques?, Int. J. Pharm. 626 (2022). https://doi.org/10.1016/j.ijpharm.2022.122157.

[46] J. Skowyra, K. Pietrzak, M.A. Alhnan, Fabrication of extended-release patient-tailored prednisolone tablets via fused deposition modelling (FDM) 3D printing, Eur. J. Pharm. Sci. 68 (2015) 11–17. https://doi.org/10.1016/j.ejps.2014.11.009.

[47] P.K. Nukala, S. Palekar, N. Solanki, Y. Fu, M. Patki, A.A. Shohatee, L. Trombetta, K. Patel, Investigating the application of FDM 3D printing pattern in preparation of patient-tailored dosage forms, J. 3D Print. Med. 3 (2019) 23–37. https://doi.org/10.2217/3dp-2018-0028.

[48] M. Fanous, M. Bitar, S. Gold, A. Sobczuk, S. Hirsch, J. Ogorka, G. Imanidis, Development of immediate release 3D-printed dosage forms for a poorly water-soluble drug by fused deposition modeling: Study of morphology, solid state and dissolution, Int. J. Pharm. 599 (2021) 120417. https://doi.org/10.1016/j.ijpharm.2021.120417.

[49] A. Goyanes, P. Robles Martinez, A. Buanz, A.W. Basit, S. Gaisford, Effect of geometry on drug release from 3D printed tablets, Int. J. Pharm. 494 (2015) 657–663. https://doi.org/10.1016/j.ijpharm.2015.04.069.

[50] W. Kempin, V. Domsta, G. Grathoff, I. Brecht, B. Semmling, S. Tillmann, W. Weitschies, A. Seidlitz, Immediate Release 3D-Printed Tablets Produced Via Fused Deposition Modeling of a Thermo-Sensitive Drug, (2018).

[51] M. Alhijjaj, P. Belton, S. Qi, An investigation into the use of polymer blends to improve the printability of and regulate drug release from pharmaceutical solid dispersions prepared via fused deposition modeling (FDM) 3D printing, Eur. J. Pharm. Biopharm. 108 (2016) 111–125. https://doi.org/10.1016/j.ejpb.2016.08.016.

[52] A.G. Crișan, S. Iurian, A. Porfire, L.M. Rus, C. Bogdan, T. Casian, R.C. Lucacel, A. Turza, S. Porav, I. Tomuță, QbD guided development of immediate release FDM-3D printed tablets with customizable API doses, Int. J. Pharm. 613 (2022). https://doi.org/10.1016/j.ijpharm.2021.121411.

[53] G. Kibria, M.A. Roni, M.S. Absar, R.U. Jalil, Effect of plasticizer on release kinetics of diclofenac sodium pellets coated with eudragit RS 30 D, AAPS PharmSciTech. 9 (2008) 1240–1246. https://doi.org/10.1208/s12249-008-9163-4.

[54] S. Obeid, M. Madžarević, M. Krkobabić, S. Ibrić, Predicting drug release from diazepam FDM printed tablets using deep learning approach: Influence of process parameters and tablet surface/volume ratio, Int. J. Pharm. 601 (2021). https://doi.org/10.1016/j.ijpharm.2021.120507.

[55] H. Liu, P. Wang, X. Zhang, F. Shen, C.G. Gogos, Effects of extrusion process parameters on the dissolution behavior of indomethacin in Eudragit ® E PO solid dispersions, Int. J. Pharm. 383 (2010) 161–169. https://doi.org/10.1016/j.ijpharm.2009.09.003.

7. Abbreviations

API: active pharmaceutical ingredient
ASD: amorphous solid dispersions
AV: acceptance value
BCS: Biopharmaceutical Classification System
CBD: cannabidiol
EPO: Eudragit®EPO
FDA: Food and Drug Administration
FDM: fused deposition modeling
HME: hot-melt extrusion
HPLC: high-performance liquid chromatography
IR: immediate release
PEO: Polyox®N10
SA/V: surface-to-volume
TGA: thermogravimetric analysis
TS: tensile strength

Appendices

Evaluation of degradation temperature of raw materials:

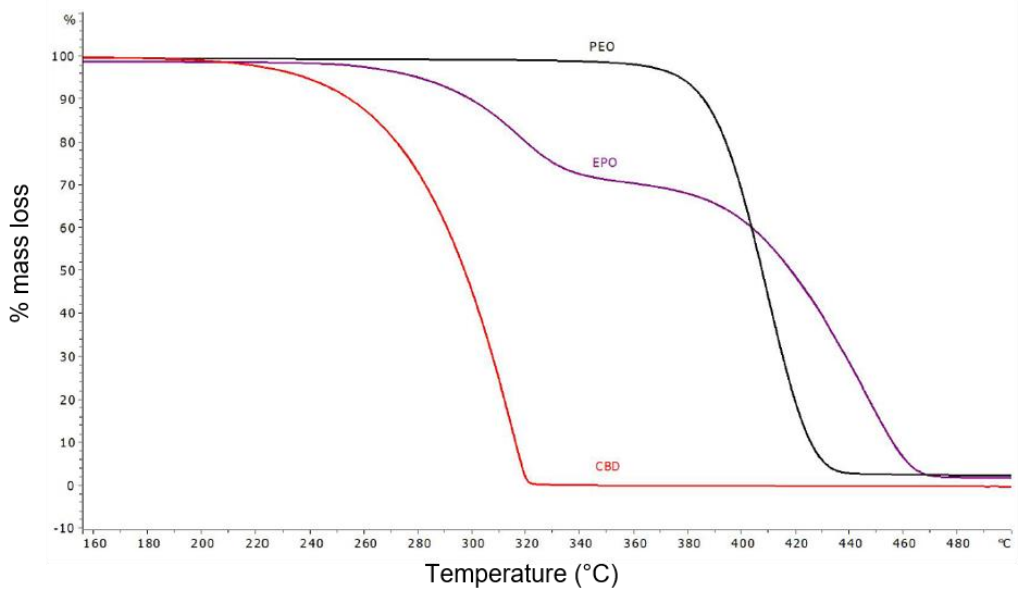

Appendix 1 - TGA curves of raw cannabidiol, Eudragit®EPO and Polyox®N10.

Appendix 1 shows that the mass loss of CBD starts at 220 °C while mass loss for EPO and PEO starts at 289 and 389 °C, respectively.

Appendix 2 shows the temperatures at which each raw material has lost 10% from the initial mass: 250 °C, 300 °C and 373 °C for CBD, EPO and PEO, respectively.

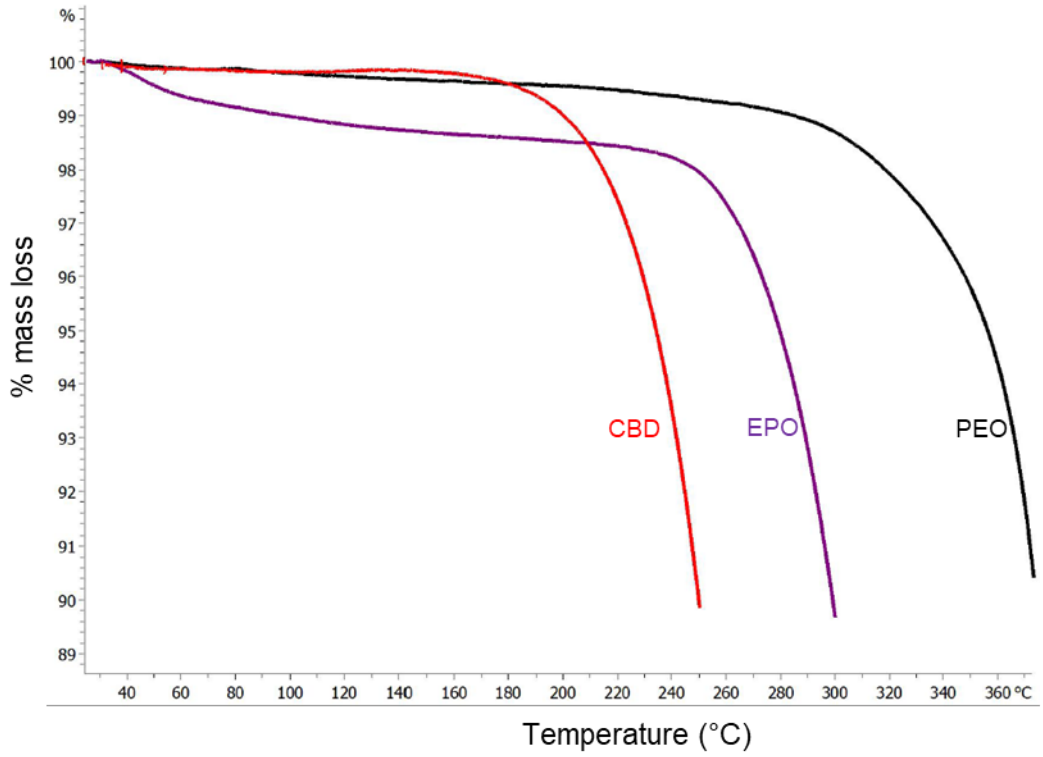

Appendix 2 – Zoom on mass loss from 100% to 90% of the initial mass for CBD, EPO and PEO